Navigating uncertainty for informed policy: the case of energy transition scenarios

M. Palucci[a,b], J.M. Tardif[b], V. Medici[b]

[a]*Reliability and Risk Engineering, Institute of Energy and Process Engineering, Department of Mechanical and Process Engineering, ETH Zurich, Leonhardstrasse 21, Zurich, 8092, Switzerland*
[b]*ISAAC, SUPSI, Via Flora Ruchat-Roncati 15, Mendrisio, 6850, Switzerland*

Abstract

Energy systems modeling and scenario development play vital roles in quantitatively assessing potential trajectories for energy transitions and informing policy decisions. Traditional frameworks often overlook uncertainties inherent in long-term projections. Addressing factors like technological progress, societal preferences, climate dynamics, and political priorities introduces complexity and deep uncertainties into energy models, leading to a wide range of computed scenarios. Uncertainty has been recognized as a significant challenge in modeling, prompting the exploration of methodologies to systematically expose and analyze uncertainties. This paper presents the use of a System Dynamics simulation model designed to perform what-if analysis for energy policies, emphasizing the importance of sensitivity and uncertainty analysis. The model is demonstrated through a case study on decarbonization in the residential sector of a Swiss canton. The framework here presented integrates a bottom-up hybrid modeling approach, global sensitivity analysis, and uncertainty analysis techniques to systematically explore uncertainties and their implications for informing policy. Results highlight the significant impact of input parameter uncertainty on model outcomes, emphasizing the necessity of considering uncertainties in decision-making processes. By employing scenario analysis and clustering techniques, the study identifies critical policy levers that can steer the residential sector toward sustainable energy transitions, offering valuable insights for policymakers and stakeholders.

Nomenclature

Abbreviations

AIC	Akaike Information Criterion
BIC	Bayesian Information Criterion
BLM	Binary logit model
CGE	Computable General Equilibrium
CLD	Causal loop diagram
DFH	Dual-family house
DH	District Heating
DHW	Domestic hot water
DSO	Distribution system operator
EH	Electric heater
EMA	Exploratory Modelling and Analysis
ESOM	Energy Systems Optimization Model
GHG	Green House Gasses
GMM	Gaussian Mixture Model
HP	Heat pump
HS	Heating solution
IAM	Integrated Assessment Model
MFH	Multi-family house
MNL	Multinomial logit
NPV	Net Present Value
OAT	One at a Time
PRIM	Patient Rule Induction Method
PV	Photovoltaic
RBD	Register of buildings and dwellings

SD	System dynamics
SFH	Single-family house
SH	Space heating
ST	Solar Thermal

Indices

i	Buildings archetype
j	Heating solution
t	Time

Symbols in equations

β_i	Coefficients used in PV probability of adoption
δ	Decay rate of people considering PV
ϵ	Share of suitable roofs to install PV
γ_i	Coefficients used in HP probability of adoption
λ^{HS}	Heating solution utility
λ^{PV}	PV utility
ν	Share of people considering installing PV
ω	Initial share of people considering PV
ϕ	Growing rate of people considering PV
ρ^{HS}	Probability of adoption HS
ρ^{PV}	Probability of adoption PV
τ	New adoptions heating solution
θ_i	Coefficient varied in Morris SA
υ^{HS}	HS peer effect
υ^{PV}	PV peer effect
B	Buildings
B^{PV}	Buildings with PV installed
EE	Elementary Effect
I^{PV}	Buildings installing PV
L	Lifetime
PHS	Primary houses share
T	Total new adoptions per archetype

1. Introduction

Energy systems modelling and scenario development are valuable tools for quantitatively assessing potential trajectories and informing policy makers [1][2]. Among the prevalent computational modelling approaches, Energy System Optimization Models (ESOM) [3][4], Computable General Equilibrium (CGE) models [5], and Integrated Assessment Models (IAMs) have been extensively utilized in energy transition scenario assessments [6]. Traditionally, these models have often employed deterministic methodologies, offering single optimal solutions or limited pathways while overlooking uncertainties inherent in long-term projections [7]. Yet, incorporating factors such as technological progress, societal preferences, climate dynamics, and political priorities into energy models introduces complexity and (deep) uncertainties [8][9][10]. Moreover, the diversity in model structures, objectives, parameterization, and spatio-temporal resolution results in a wide range of computed scenarios [11]. Aware of the interface between models and policy-making, uncertainty has been identified as a critical challenge in modelling scenarios [12]. So far, layers of complexity have gradually been added to models, allowing for the observation of more accurate phenomena, but not necessarily helping decision-makers decipher the inherent uncertainties [12] [13]. The accumulation and opaqueness of uncertainties and the potential divergences in outcomes of models could potentially mislead decision-makers [3], hinder consensus [14], and undermine confidence in model-based decision-making.

Recent studies have identified a few prominent trends in response to these limitations concerning to complexity and uncertainty. Firstly, using methods to explore broader solution spaces systematically can offer a diversity of design options that expose trade-offs vital in informing politically difficult decisions [15]. Secondly, multi-method linking and multi-model comparison permit a large scenarios ensemble analysis that can capture a broad uncertainty range [12][16][17]. Lastly, advanced sensitivity and uncertainty analysis methods have gained traction as a means to qualify the substantial uncertainties in model inputs, structure, and outputs [18].

On the one hand, System dynamics (SD) is well suited to model the complexity that arises due to interconnected systems with feedback mechanisms and non-linearity, and has been used as a decision support method in the energy sector [19]. On the other hand, as presented in a review by [20], while traditional SD implicitly deals with uncertainty, most studies rarely ex-

plicitly and systematically tackle the uncertainty in their inputs and model, and the sensitivity of the results to these elements.

Sensitivity analysis evaluates the response of the model to variations in inputs or parameters, identifying influential factors. Advanced methods, such as variance-based sensitivity analysis, are commonly employed to determine sensitivity. Uncertainty, stemming from input reliability, parameter variability, or structural uncertainties, necessitates quantitative analysis to gauge model prediction reliability. Techniques like Monte Carlo simulation, Bayesian inference, stochastic programming, robust optimization, and the Patient Rule Induction Method (PRIM), have been used to reflect complex system dynamics in uncertain transition scenarios and provide insights into model robustness[8][3]. Some notable computational SD modeling frameworks have incorporated such techniques to systematically and transparently expose uncertainty. For example, in [21] is presented the a system dynamic model of the UK energy system where a stochastic Monte Carlo approach is used to capture parametric uncertainty and potential pathway variations resulting from technological, economic, and behavioural uncertainty. The SD based tool EnROADS [22] offers an interactive exploration of a broad solution space for a global energy transition, where the end-user can view the varying outcomes when adjusting inputs. The study by [23] presents a comprehensive multi-method approach combining System Dynamics and Exploratory Modeling and Analysis (EMA) to explore and analyze uncertain dynamics and test policy robustness. The EMA workbench [24] used by the authors offers a methodological approach to explore the consequences of the various uncertainties for decision making and allows a systematic exploration of a large ensemble of scenarios.

This paper will describe a new SD simulation model that allows to investigate what-if scenarios [25], in the context of energy policy. We showcase the importance of the sensitivity and uncertainty analysis in a case study for the decarbonization of the residential sector in a Swiss canton. The results therefore emphasise the necessity of such analysis for informing policy. The Methodology section of the paper will first presents the SD model which adopts concepts of bottom-up hybrid modeling approaches [26] as it simulates decisions taken by representative agents, thereby allowing to evaluate the effect of different policies on specific population clusters. This is followed by the presentation of the uncertainties and the methods employed to assess them. The Results section will focus on the outcomes of the uncertainty analysis, and the Discussion section will focus on the potential implications for informing policy makers.

2. Methodology

This Section is divided in two parts: in the first, the co-adoption model of Photovoltaic (PV) and Heat Pump (HP) is presented; in the second, the main uncertainties related to the model are described. This is followed by an illustration of the methodology used to address these uncertainties and derive policy relevant considerations.

2.1. PV and HP co-adoption model

Switzerland is actively pursuing a sustainable transformation in its electricity sector, aligning with the Paris Agreement to achieve net-zero greenhouse gas emissions. In order to pursue its goal for the year 2050 [27], a fundamental role is played by the emissions reduction in the residential sector [28]. In this context, achieving sustainability targets hinges on embracing distributed electricity production, particularly through PV [29], and renewable-based heating technologies like heat pumps for residential heating [30]. This paper introduces a model tailored to this context, enabling the simulation of long-term adoption for both PV and HP in residential buildings. Unlike conventional methods that focus solely on individual technology adoption, our framework considers the correlations between PV and HP adoption. The model is developed in Vensim [31] and exemplified with the case study of Ticino, a Canton in southern Switzerland, but, since it relies on open data, it can be extended to the entire country.

2.1.1. Model description

The Ticino regional model for co-adoption of PV and HP technologies within the residential sector is conceptually depicted in the Causal Loop Diagram (CLD) shown in Figure 1. This graphical representation illustrates the qualitative relationships between key stocks and drivers influencing the evolution of PV and HP adoption. The image highlights two primary stocks of interest: “PV Buildings” and “HP Buildings”, with the feedback loops involved denoted as reinforcing (R) and balancing (B).

Reinforcing loops R1 and R2 show the influence of peer effects: if the presence of a given technology increases, it enhances its social appeal, leading to further adoption. Conversely, balancing loops B1 and B2 reflect the finite pool of buildings eligible for PV or HP adoption, wherein increased adoption diminishes

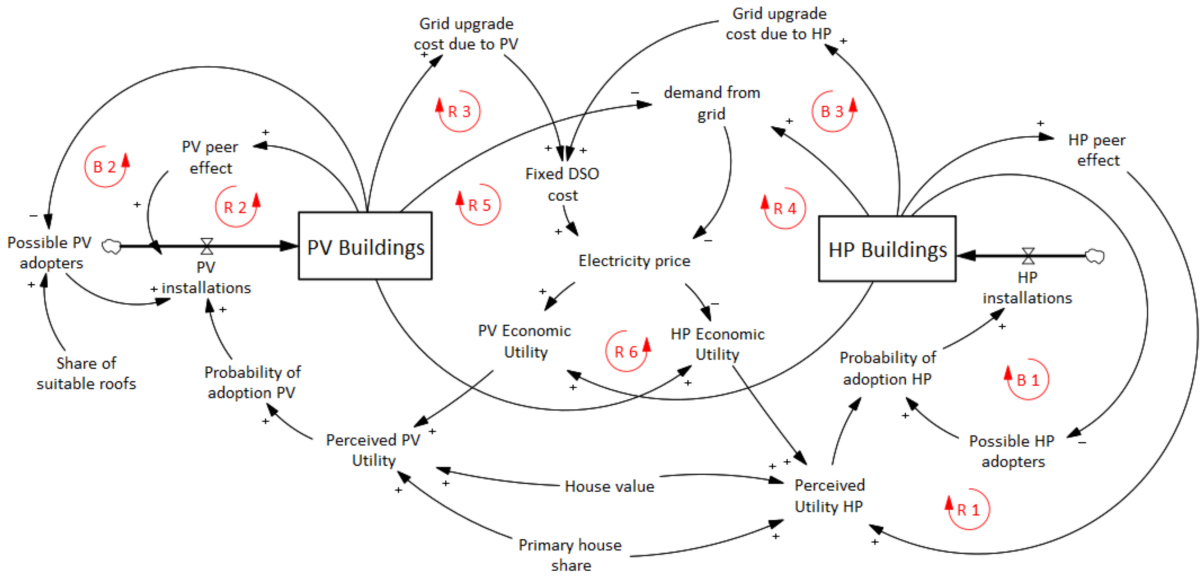

Figure 1: Causal Loop Diagram representing the main variables of the SD model.

the pool of potential adopters. Loops B3 and R3 delineate the impact of PV and HP adoption on grid-related costs, influencing the economic attractiveness of each technology. Specifically, increased HP adoption leads to heightened grid reinforcement costs, resulting in decreased economic utility for HP installations (B3), while PV deployment reduces total electricity demand, leading to higher electricity prices and increased economic appeal for PV installations (R3).

Further reinforcing loops, R4 and R5, elucidate the effects of HP and PV deployment on total electricity demand. As more HP systems are adopted, electricity demand increases, and, since it is assumed that the DSO annual costs are fixed, this leads to a decrease in electricity prices and higher HP economic viability (R4). Conversely, PV deployment decreases total electricity demand, causing electricity prices to rise and amplifying the attractiveness of PV installations (known as the Death Spiral phenomenon [32] - R5). Finally, reinforcing loop R6 captures the technical synergies between PV and HP systems, considering that the installation of one technology enhances the economic appeal of the other. Specifically, the presence of a HP system in a building increases the economic viability of installing a PV system, while buildings already equipped with PV systems find HP solutions more economically attractive compared to traditional heating options.

2.1.2. Building archetypes definition

The model simulations start from the year 2023, using data extracted from public databases to characterize the initial state of the residential building stock in Ticino. Key datasets used include:

- Register of Buildings and Dwellings (RBD) [33]: This repository furnishes essential information concerning building attributes such as size, type, construction period, and the installed heating solution.
- Electricity Production Plants [34]: This database offers insights into the PV plants located within the canton, encompassing details such as installation year, location, and installed capacity.
- Suitability of Roofs for Solar Power [35]: Utilized to estimate the solar photovoltaic potential of buildings, this dataset categorizes building roofs into sub-surfaces graded on their suitability for solar energy production, denoted on a scale from 1 (lowest adequacy) to 5 (highest). The share of roofs suitable for PV installation is determined as the ratio of areas with adequacy scores equal to or exceeding 3.

The categorization based on building construction periods is replaced with a classification grounded in building energy efficiency, to simplify the model and reduce the categories considered in buildings segmentation. Given the well-established correlation between

building construction periods and their efficiency [36], we considered the specific Space Heating (SH) consumption data from [37], and computed total annual SH demand for the residential sector. Then, we computed the share that from each construction period (nine construction periods reported in the RBD) belongs to each energy performance category (five energy performance categories assumed). After that the specific SH consumption is computed and serves as a model input. The resulting SH annual specific consumption is reported in Table A.5. To sum up, based on the information from the three databases mentioned above, buildings are segmented based on the following characteristics:

- Building properties: comprehending details such as size (A: < 150 m^2; B: 150-300 m^2, C: < 300 m^2), type (Single-Family House [SFH], Dual-Family House [DFH], Multi-Family House [MFH]), and energy efficiency levels (ranging from Very Low to Very High).
- Building location: buildings are categorized based on their district of residence, including Vallemaggia, Mendrisio, Bellinzona, Leventina, Blenio, Lugano, Riviera, and Locarno. The considered districts differ not only for the building archetypes proportions, but also for climate conditions, that are considered in the computation of the annual heating demand per building.
- PV presence: buildings are divided according to the presence or absence of PV.
- Heating Solution (HS): further subdivision is performed based on 15 potential heating solutions for SH and Domestic Hot Water (DHW), as delineated in Table 2.

This segmentation (shown in Table 1 and 2) results in a total of 360 distinct combinations of building physical attributes (size, type, performance, and district), referred to as building "archetypes". When considering the additional combinations arising from heating solutions and PV presence, the total possible building segments amount to 10'800. This framework provides the possibility to explore possible future developments of the residential sector in terms of both aggregate outcomes and more specific results per building typology.

2.1.3. Main equations

The PV installations within the residential sector is influenced by a multitude of factors, extending beyond purely techno-economic considerations. In our proposed model, as depicted in Figure 1, three key determinants are employed to calculate the perceived utility associated with PV installation:

$$\lambda_{t,i}^{PV} = \beta_{0,i} + \beta_1 \cdot Eco_{t,i} + \beta_2 \cdot PHS_i + \beta_3 \cdot Val_i \quad (1)$$

Here, t denotes the time step at which the perceived utility is evaluated, and i represents the single building archetype. The β coefficients represent the weights assigned to each determinant influencing the perceived utility, which are determined through calibration using historical data. The significance of the determinants is outlined as follows:

- Eco - Economic Utility: this is the Net Present Value (NPV) computed for the possibility of installing PV. The computation is stratified by building type, size, performance, and the installed heating solution. It considers also all the incentives in force.
- PHS - Primary House Share: Ticino is one of the Swiss cantons with the highest share of secondary houses; the share is computed based on [38] for each District. The high PV installation costs and the policy framework in Ticino favoring self-consumption, decrease the probability of installing a PV in secondary houses.
- Val - House Value: This factor reflects the likelihood of PV installation based on the premise that if the investment cost of PV installation constitutes a significant portion of the house value, the decision to install PV becomes less probable. This computation is differentiated by building performance category, and the coefficients utilized as input, are derived from correlations between house age and its value in the Swiss residential property model price index [39].

The perceived PV utility $\lambda_{t,i}^{PV}$ is used to compute the probability of PV adoption $\rho_{t,i}^{PV}$ according to a Binary Logit Model [40]:

$$\rho_{t,i}^{PV} = \nu_t \frac{1}{1 + e^{-\lambda_{t,i}^{PV}}} \quad (2)$$

Where ν_t is the share of people considering PV installation, which varies between 0 to 1 and evolves driven by PV peer effect υ_t^{PV}, computed as the share of buildings with a PV already installed:

$$\nu_t = \nu_{t-1} + \upsilon_t^{PV} \cdot \phi \cdot (1 - \nu_t) - \delta \cdot \nu_t \quad (3)$$

Size [m^2]	Type	PV Presence	Performance	District
≤ 150 (A) 150-300 (B) > 300 (C)	Single Family House Dual Family House Multi Family House	PV yes PV no	Very Low Low Moderate High Very High	Vallemaggia Mendrisio Bellinzona Leventina Blenio Lugano Riviera Locarno

Table 1: Categories that define the single building archetype

Name	Explanation	Name	Explanation
1 - Oil Boiler	SH & DHW	9 - Heat Pump	SH & DHW
2 - Gas Boiler	SH & DHW	10 - Oil & HP	Oil: 75%(SH & DHW) HP: 25%(SH & DHW)
3 - Wood Boiler	SH & DHW	11 - Gas & HP	Gas: 75%(SH & DHW) HP: 25%(SH & DHW)
4 - EH	SH & DHW	12 - HP & ST	HP: SH ST: DHW
5 - Oil & EH	Oil: SH EH: DHW	13 - Oil & ST	Oil: SH ST: DHW
6 - Gas & EH	Gas: SH EH: DHW	14 - Gas & ST	Gas: SH ST: DHW
7 - Wood & EH	Wood: SH EH: DHW	15 - Pellet & ST	Pellet: SH ST: DHW
8 - Pellet	SH & DHW		

Table 2: Considered heating solutions; each solution is a combination of one or more heating technologies. It is also indicated the utilization of the considered technology. For example the solution "Oil & ST" has oil boiler for space heating (SH) and solar thermal collectors for domestic hot water (DHW)

$$\upsilon_t^{PV} = \frac{B_t^{PV}}{B_t} \tag{4}$$

In this way, the buildings installing PV $I_{t,i}^{PV}$ is computed considering the share of suitable roofs ϵ_i and the buildings that have already installed it $B_{t,i}^{PV}$:

$$I_{t,i}^{PV} = (B_{t,i} \cdot \epsilon_i - B_{t,i}^{PV}) \cdot \rho_{t,i}^{PV} \tag{5}$$

Also in the case of heating solutions, several factors affect the decision. Being this decision between several possible heating solutions (see Table 2), a Multinomial Logit (MNL) model [41] is used to examine the likelihood of opting for a specific heating solution from a choice set comprising more than two alternatives. For a given building archetype i, where the choice is between j possible solutions, the perceived utility at each time t is given by:

$$\lambda_{t,i,j}^{HS} = \gamma_{0,i} + \gamma_1 \cdot Eco_{t,i,j} + \gamma_2 \cdot Val_i + \gamma_3 \cdot \upsilon_{t,j}^{HS} + \gamma_4 \cdot G_j \tag{6}$$

Where the Eco variable represents the NPV associated to the j heating solution; the Val is assumed to affect the solutions going from 8 to 15 in Table 2, which are the renewable based solutions and are characterized by a higher investment cost. Moreover, for the perceived utility computation, two more factors are considered compared to the PV case. The first is peer effect υ_j^{HS}, computed as the share of buildings with the heating solution j already installed; it is found that adding it to the perceived utility calculation, improves the model capability to replicate historical trends in the calibration. The second one is the G (Green utility), which is simply computed as the overall GHG emissions associated to the j HS considered. So, the probability of adopting a HS j is computed according to the MNL framework:

$$\rho_{t,i,j}^{HS} = \frac{e^{\lambda_{t,i,j}^{HS}}}{\sum_j e^{\lambda_{t,i,j}^{HS}}} \tag{7}$$

It is also assumed that buildings substitute their heating solution j when its lifetime L_j comes to end. So, at each time step t, the total new adoptions $T_{t,i}$ for building archetype i and the new adoptions $\tau_{t,i,j}$ per heating solution j are computed as:

$$T_{t,i} = \sum_j \frac{B_{t,i,j}}{L_j} \tag{8}$$

$$\tau_{t,i,j} = T_{t,i} \cdot \rho_{t,i,j}^{HS} \tag{9}$$

The data on technology used in the model, comprehending both phisycal properties and costs are reported in Appendix A.

2.1.4. Calibration

Model calibration is fundamental to assure that its behavior is consistent with the phenomenon it is representing. In this context, the focus lies on analyzing the prospective deployment of HP and PV within the cantonal residential sector. The calibration process entails adjusting the probabilities of PV and HP adoption across various building categories to match historical

Parameter	Range	Explanation
Renovation Rate	0.2% - 5%	Expressed as a share of total buildings.
Construction Rate	0.8% - 1.2%	Expressed as a share of total buildings.
Demolition Rate	0.4% - 0.6%	Expressed as a share of total buildings.
Population	0% - 10%	Share of population decrease in 2050. It affects the share of primary houses.
Compensation price PV	0.04 - 0.23 CHF/kWh	Compensation for the electricity injected in the grid.
PV Grant	50% - 150%	Parameter multiplied by the actual PV grant, expressing uncertainty on possible future changes in this parameter.
HP Grant	50% - 150%	Parameter multiplied by the actual HP grant.
ST Grant	50% - 150%	Parameter multiplied by actual grant for Solar Thermal collectors.
Pellet Grant	50% - 150%	Parameter multiplied by the actual Pellet grant.
Year stop PV incentives	2030 - 2050	Year in which the incentives for PV will stop.
Year stop HS incentives	2030 - 2050	Year in which the incentives for the heating solutions will stop.
DH uncertainty	0.065 - 0.468	Input parameter in the model proportional to the District Heating (DH) diffusion. 0.065 corresponds to a share of buildings connected to DH in 2050 of 5%, 0.468 corresponds to a share of 25%.
New buildings PV obligation	0.8 - 1.2	A law in the canton states that all new buildings have to produce electricity (installing a PV) "unless economically unfeasible". This uncertainty in considered in the model assuming that for each archetype the share of buildings forced to install a PV is equal to the share of buildings with at least moderate potential according to [42]. This value is then multiplied for each archetype by this parameter ranging from 0.8 to 1.2.
PV cost reduction	21% - 64%	PV capital cost reduction by 2050.
HP cost reduction	11% - 34%	HP capital cost reduction by 2050.
ST cost reduction	26% - 79%	ST capital cost reduction by 2050.
Oil cost increase	0 - 0.12 CHF/kWh	Oil cost increase by 2050.
Gas cost increase	0 - 0.31 CHF/kWh	Gas cost increase by 2050.
Pellet cost increase	0 - 0.21 CHF/kWh	Pellet cost increase by 2050.

Table 3: Deep uncertainties considered in the exploratory analysis.

adoption patterns spanning from 2011 to 2023. During calibration, the following parameters are adjusted to align the model output to observed historical data:

- β coefficients used to compute the perceived utility of PV installation (see Eq. 1). The β coefficients calibrated are 23 (see Table B.8a).
- γ coefficients used to compute the perceived utility of HP installation (see Eq. 6). The γ coefficients calibrated are 23 (see Table B.8b).
- Coefficient ϕ and δ in Equation 4. Also a coefficient called ω, which represents the initial share of people considering PV (in 2011) is calibrated (see Table B.8c)

Thus, the calibration seeks to optimize the normal log likelihood:

$$max \left\{ - \ln \frac{1}{\sigma \sqrt{2\pi}} e^{-\left(\frac{y-\hat{y}}{\sigma}\right)^2} \right\} \tag{10}$$

Where, y represents the adoption probabilities computed by the model, while $\hat{y}$ are the adoption probabilities derived from historical data. Calibration is conducted for the mean adoption probabilities of PV and HP across different building categories (including size, type, performance, and district) from 2011 to 2023, leading to 480 observations and involving 49 calibrated parameters. The resulting parameters, along with their 99% confidence intervals, are detailed in Table B.8a, Table B.8b and Table B.8c; additionally, Table B.8d displays the resulting r^2 for the respective variables of interest, indicating a satisfactory model fit overall.

2.2. Model uncertainties

Exploring the future trajectories of the Ticino residential sector entails dealing with various forms of uncertainty. Within the literature, diverse typologies of uncertainties have been delineated. For instance, [43] distinguishes between stochastic and real uncertainty, where the former encompasses subjective and frequency-based probabilities, while the latter pertains

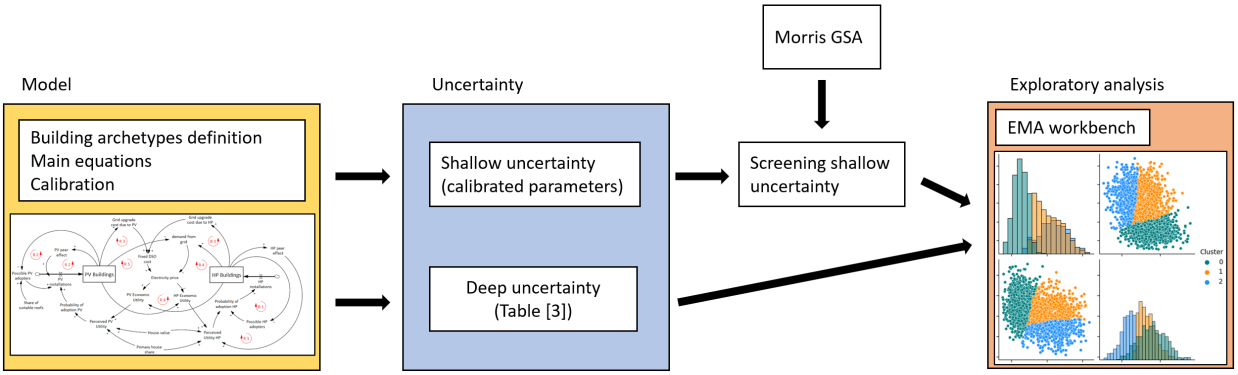

Figure 2: Description of the step-by-step methodology to address model uncertainties.

to the future states of the considered phenomena resulting from the behavior of other actors. A study by [44] further refines this classification, distinguishing between uncertainties that can be treated with probabilities and those that cannot. Uncertainties falling into the latter category are commonly referred to as deep uncertainty [45]. Here, deep uncertainty denotes a scenario wherein multiple possibilities exist without clear ranking in terms of plausibility.

In the presented model, we categorize uncertain input parameters into two primary groups. The first group encompasses uncertainties associated with model-calibrated parameters, classified as "shallow uncertainties" according to [45]. These uncertainties allow the use of distribution probabilities to describe the plausibility of uncertain events. The second group, outlined in Table 3, comprehends deep uncertainties.

To address these uncertainties in the proposed model, we followed the framework reported in Figure 2. Since our objective is to conduct an analysis that explores a spectrum of potential trajectories for the future evolution of the Ticino residential sector and, given the multitude of uncertain parameters inherent in a hybrid model involving 10'800 building segments, as presented here, we opt to reduce the computational burden and complexity during exploratory analysis by reducing the number of calibrated parameters part of the analysis. To achieve this, we employ the Morris Global Sensitivity Analysis (GSA) screening method, which offers an efficient means of identifying influential factors and prioritizing them for further analysis. Specifically, the Morris method [46] assesses the importance of calibrated parameters on model outputs, allowing us to highlight a selected group of parameters that show the most significant impact on model outcomes. It is demonstrated that the method is effective in identifying the few important factors in a model that contains many factors [47]; at the same time, compared to other more sophisticated techniques for GSA to rank or screen input parameters, such as the Sobol method [48], it allows to perform the analysis with a lower number of total evaluations, which results in a lower computational cost.

One of the parameters computed following the Morris GSA method is the elementary effect EE, which represents the change in model output resulting from perturbing a single input parameter while keeping all other parameters fixed. This value is used to compute the two outcomes of interest: μ^* and σ (see the Appendix C for the detailed explanation of how this outcomes are computed). The first represents the average absolute value of the elementary effects calculated for a specific input parameter. It provides a measure of the overall sensitivity of the model output to variations in that parameter; while the second represents the standard deviation of the elementary effects calculated for the same input parameter. It quantifies the variability or dispersion of the elementary effects around their mean value. Together, μ^* and σ help characterize the sensitivity of the model to different input parameters, with μ^* indicating the average impact and σ providing information about the variability of that impact. In our analysis, we screened the calibrated 49 parameters based on their effect on PV and HP probabilities of adoption. The Morris method is a semi-quantitative approach for factor screening; for this reason, there is no definitive boundary separating the important and irrelevant input parameters [47]. Moreover, in most of the models with a large number of parameters, such as the one here considered, it turns out that only few inputs are really influential on the output, while many are irrelevant and some are in between [47]. For this reason, in practice, a demarcation line separating influential and irrelevant parameters can often be drawn qualitatively. In this study, only the inputs with at least one between μ^* and σ higher then 10% are

considered influential and thus varied in the exploratory analysis; this threshold was already employed in previous screening analysis using the Morris method on SD models [49]. The inputs with both μ^* and σ lower than 10% are kept constant to their optimal value during the exploratory analysis.

Following the identification of the most influential calibrated parameters, an exploratory analysis is conducted using the Exploratory Modeling Workbench [24]. This analysis proceeds through the following steps:

- 2'000 scenarios are simulated by varying the selected uncertain parameters using the EMA workbench, sampling over both the calibrated parameters post-Morris screening and the parameters within the deep uncertainty group. The calibrated parameters post-Morris screening are sampled in the input space resulting from the 99% confidence intervals reported in Table B.8; the parameters within the deep uncertainty group are sampled in the range indicated in Table 3. The outcomes are recorded in terms of the final (year 2050) proportion of buildings with HP installations and total PV production.
- Clusters of results exhibiting similar outcomes are delineated using a Gaussian Mixture Model (GMM), a probabilistic model leveraging a mixture of Gaussian distributions [50]. The number of clusters is determined based on Bayesian Information Criterion (BIC) and Akaike Information Criterion (AIC) considerations, resulting in three distinct clusters.
- A detailed examination of these clusters is undertaken using the Patient Rule Induction Method (PRIM) [51], facilitating the identification of uncertainty ranges in input parameters that lead to specific outcomes.
- The findings of the PRIM analysis are subjected to analytical scrutiny, yielding insights with policy implications.

3. Results

The outcomes of the Morris screening method are summarized in Table 4, which shows the μ^* and σ computed with respect to the probabilities of PV and HP adoptions. Following the screening process, we decided to include in our exploratory analysis input parameters exhibiting a μ^* or σ of at least 10%. This refinement led to a reduction in the number of parameters considered for exploration from 49 to 13 (parameters with the (*) after the name in Table 4).

Parameter	μ^* - PV	σ - PV	μ^* - HP	σ - HP
δ (*)	10.5	0.6	0.05	0.01
ϕ	7.9	1.2	0.04	0.01
ω	5.0	0.7	0.06	0.01
β_1 (*)	13.1	2.5	0.05	0.01
β_2 (*)	10.6	1.7	0.04	0.01
β_3	7.9	1.6	0.04	0.01
β_0 (*)	10.2	1.8	0.04	0.01
$\beta_{0,Vallmaggia}$	0.9	0.2	0.01	0.00
$\beta_{0,Mendrisio}$	5.3	0.7	0.02	0.01
$\beta_{0,Bellinzona}$	7.3	1.6	0.03	0.01
$\beta_{0,Leventina}$	1.5	0.5	0.01	0.00
$\beta_{0,Blenio}$	1.8	0.5	0.01	0.00
$\beta_{0,Lugano}$ (*)	11.0	1.6	0.05	0.02
$\beta_{0,Riviera}$	2.3	0.6	0.01	0.01
$\beta_{0,Locarno}$	7.8	1.8	0.04	0.01
$\beta_{0,VeryLow}$	5.9	0.8	0.02	0.01
$\beta_{0,Low}$	7.3	1.9	0.03	0.01
$\beta_{0,Moderate}$	9.3	1.6	0.05	0.01
$\beta_{0,High}$	7.3	0.9	0.04	0.01
$\beta_{0,VeryHigh}$	0.5	0.1	0.01	0.00
$\beta_{0,A}$	6.5	1.5	0.02	0.01
$\beta_{0,B}$ (*)	10.3	1.9	0.04	0.02
$\beta_{0,C}$	5.9	0.9	0.03	0.01
$\beta_{0,SFH}$ (*)	11.0	1.6	0.05	0.02
$\beta_{0,DFH}$	5.8	1.5	0.02	0.01
$\beta_{0,MFH}$	3.6	0.6	0.02	0.01
γ_1 (*)	0.08	0.03	11.35	2.32
γ_2	0.10	0.03	6.75	2.79
γ_3 (*)	0.09	0.05	12.28	4.06
γ_4 (*)	0.13	0.05	11.62	3.62
$\gamma_{0,Vallmaggia}$	0.01	0.01	2.08	0.69
$\gamma_{0,Mendrisio}$	0.06	0.02	5.74	1.54
$\gamma_{0,Bellinzona}$	0.08	0.03	5.31	1.46
$\gamma_{0,Leventina}$	0.03	0.02	3.29	1.75
$\gamma_{0,Blenio}$	0.03	0.01	2.35	0.87
$\gamma_{0,Lugano}$	0.11	0.03	9.70	3.22
$\gamma_{0,Riviera}$	0.06	0.02	2.42	0.81
$\gamma_{0,Locarno}$	0.08	0.03	8.94	2.32
$\gamma_{0,VeryLow}$ (*)	0.07	0.03	10.28	4.35
$\gamma_{0,Low}$	0.12	0.06	8.17	1.94
$\gamma_{0,Moderate}$	0.04	0.02	3.30	0.56
$\gamma_{0,High}$	0.18	0.06	7.53	1.29
$\gamma_{0,VeryHigh}$	0.01	0.01	0.37	0.02
$\gamma_{0,A}$ (*)	0.06	0.02	10.07	4.99
$\gamma_{0,B}$	0.13	0.04	9.48	2.57
$\gamma_{0,C}$	0.10	0.03	8.26	1.61
$\gamma_{0,SFH}$ (*)	0.13	0.04	10.91	3.20
$\gamma_{0,DFH}$	0.04	0.01	6.92	1.51
$\gamma_{0,MFH}$	0.05	0.02	6.10	1.12

Table 4: μ^* and σ (in [%]) computed with the Morris method for the 49 calibrated parameters with respect to the probabilities of adopting PV and HP. Parameters followed by the (*) are the ones selected after the screening.

Subsequently, the exploratory analysis was conducted utilizing the EMA workbench, with input parameters varied within the ranges specified in Table 3 and the selected calibrated parameters after the screening with their confidence bounds (see Table B.8a, Table B.8b and Table B.8c). Figures 3 and 4 depict the outputs obtained from 2'000 simulation runs for the two key variables under scrutiny: the proportion of residential buildings equipped with HPs and the aggregate elec-

tricity production from PV installations. These images prove the significant impact of input parameter uncertainty, as evidenced by the considerable variation in outcomes. Specifically, projections for the share of HP-installed buildings in 2050 ranges from 46% to over 70%, while expected annual PV production spans from 500 GWh to over 900 GWh.

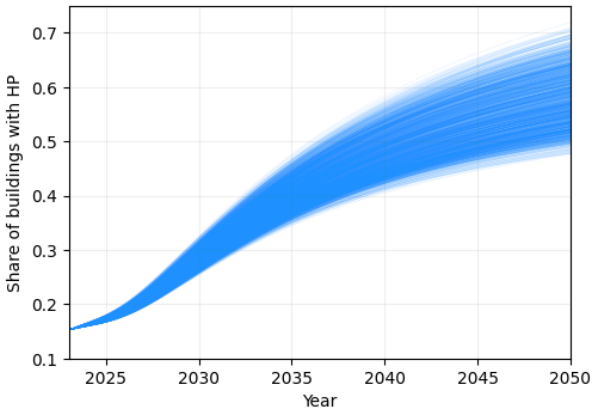

Figure 3: Results of the 2'000 runs for the share of buildings with a HP installed.

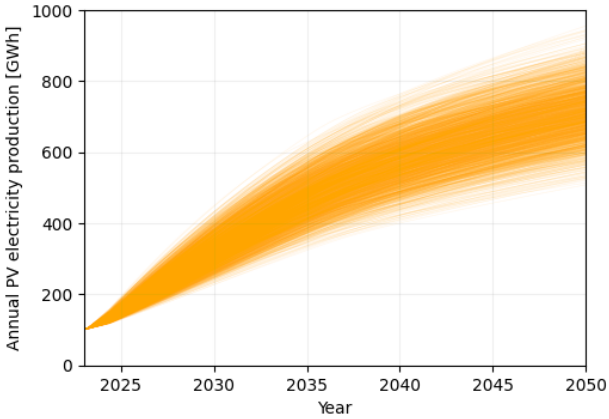

Figure 4: Results of the 2'000 runs for the total annual PV production.

Given the diverse array of outcomes for these variables of interest, a clustering approach using the GMM method facilitates further detailed analysis (see Appendix D). The number of clusters was selected to minimize both the BIC and AIC varying the number of components, resulting in the identification of three distinct clusters. The outcomes of this clustering process are illustrated in Figure 5, wherein Cluster 1 encompasses

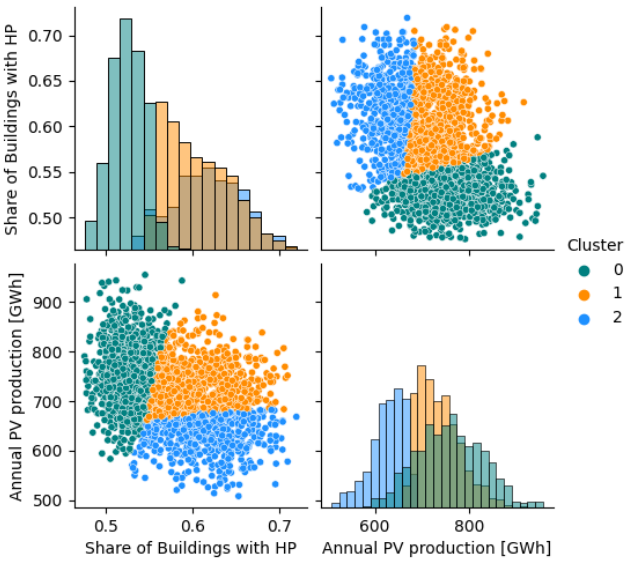

Figure 5: Resulting clusters using the GMM.

results indicative of medium to high levels of both HP adoption and PV electricity production, while Clusters 0 and 2 showcase contrasting scenarios. Specifically, Cluster 0 comprises instances where HP adoption is low but PV production varies widely, whereas Cluster 2 encompasses cases where PV production is low while HP adoption exhibits substantial variability.

Figures 6a, 6b and 6c provide insights into the results of the PRIM analysis conducted for Clusters 0, 1, and 2, respectively (see Appendix E for a more detailed explanation of the PRIM methodology). Notably, the "DH Adoption" parameter emerges as a pivotal factor significantly influencing future HP penetration rates. As delineated in Table 3, this parameter represents the considerable uncertainty surrounding the future development of District Heating (DH) networks. This factor has recently gained importance as, under the new cantonal law [42], Municipalities are granted authority to mandate building that meet certain criteria to connect to a DH network, a decision influenced by numerous uncertain variables. Consequently, DH adoption is modeled as an exogenous input parameter due to its complex and uncertain nature. Moreover, in the cantonal energy plan, it is mentioned that DH will serve approximately 25% of the heating demand, while in 2023 the share of buildings served by DH was less then 2%. The uncertainty related to this parameter deeply affects the expected HP penetration: for example, from the results for cluster 0 emerges that a low HP deployment will be present if the DH Adoption parameter is between 0.33 and 0.47 (cor-

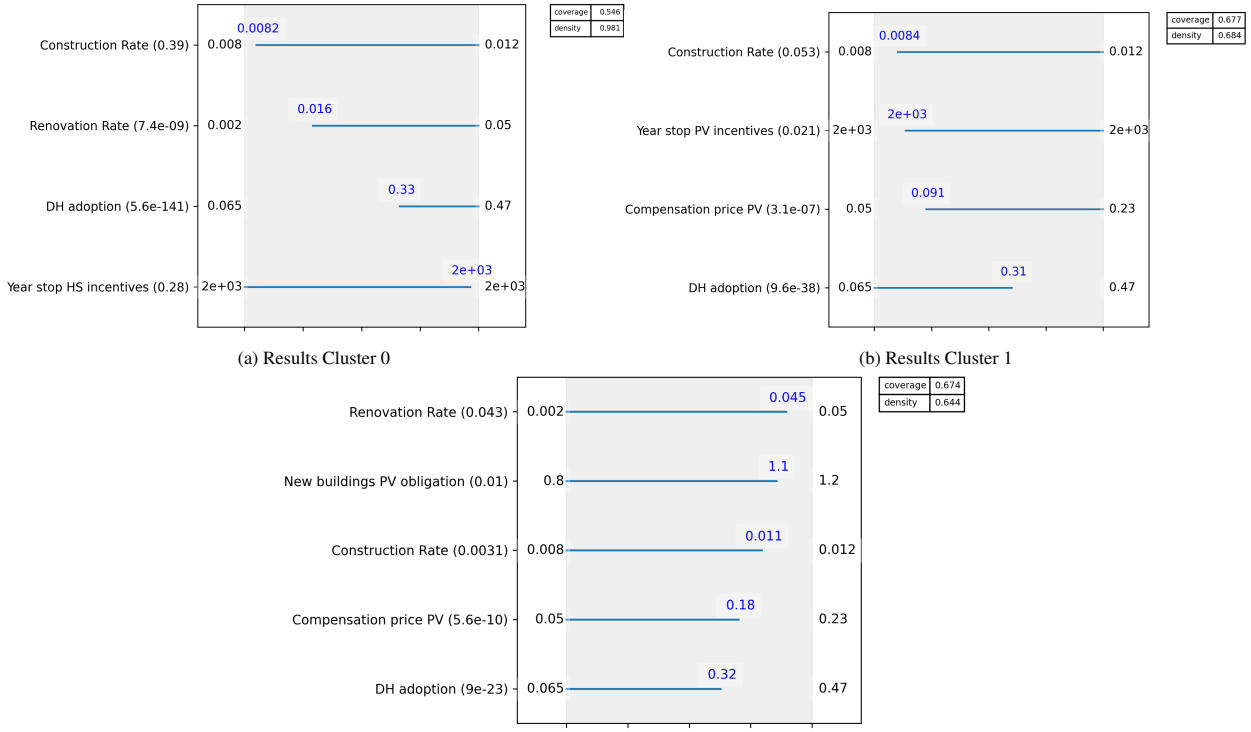

(a) Results Cluster 0

(b) Results Cluster 1

(c) Results Cluster 2

Figure 6: Representation of the PRIM analysis results for one of the points found for each the three clusters in the trade-off shown and explained in Figure E.9. On the upper right corner of each image it is indicated the coverage and density of the box here considered, but, as shown in Figure E.9, many boxes result from the analysis. Here boxes that result in a coverage higher than 0.6 and at least four input parameters found to be restricted in the analysis are considered. However, for a more comprehensive understanding of policy implications, it is recommended to conduct further PRIM analyses on multiple boxes.

responding to a share of buildings connected to DH in 2050 of 18% and 25%, respectively).

Moreover, uncertainties pertaining to future policy evolution show a significant influence, particularly on PV deployment. For instance, to align with Cluster 1 outcomes, incentives for PV installations must remain in effect until at least 2034, with remuneration for the electricity injected in the grid set at a minimum of 9 ct./kWh. Additionally, incentives for heating solutions also impact HP deployment, as evidenced by Cluster 0 results, where termination of heating solution incentives before 2048 results in diminished HP deployment. Noteworthy is the role played by uncertainties related to parameters such as Construction Rate and Renovation Rate, as observed in Cluster 0 outcomes. Scenarios characterized by renovation rates exceeding 1.6% and construction rates exceeding 0.82% tend to exhibit lower HP penetration. This is due to the cantonal regulatory framework that, in case of HS substitution, imposes to install a HS at least partially relying on renewable energy (solutions 8 to 15 in Table 2), for buildings with a low energy efficiency (Moderate to Very Low categories in Table 1); so, even though the choice for HS based on fossil fuels is low for buildings with high thermal efficiencies, it is allowed, and, in case of higher renovation rates, this could result in a slightly lower share of buildings heated by HP.

4. Conclusions

The presented study employs a comprehensive methodology to model the co-adoption dynamics of PV and HP technologies within the residential sector of the Ticino canton. By integrating a System Dynamics approach, detailed empirical data, and scenario analysis, we have shown key insights into the factors shaping the future evolution of renewable energy adoption in the region.

The regional co-adoption model developed in this study was presented with a CLD to illustrate the various factors influencing PV and HP adoption. By incorporating feedback loops, such as reinforcing effects of peer

influence and balancing effects of finite building stocks, the model captures the dynamic interplay between technological adoption, economic incentives, and regulatory policies. Additionally, the model accounts for technical synergies between PV and HP systems, highlighting the potential for mutually reinforcing adoption pathways. Moreover, through calibration, we have ensured that the model accurately replicates historical adoption trends, thus enhancing confidence in its predictive capabilities.

Uncertainty analysis reveals the inherent complexity of forecasting future adoption patterns, particularly in the context of evolving policy landscapes and technological advancements. By employing sensitivity analysis techniques, we have identified influential factors driving variations in model outcomes. Our exploration of uncertainty ranges through scenario analysis sheds light on the range of potential outcomes and the factors driving divergence among scenarios. Notably, uncertainties surrounding policy incentives for both PV and HP installations emerge as key determinants shaping future adoption trajectories, highlight once again the fundamental role that policymakers have in shaping the energy transition.

The scenario analysis conducted in this study provides policymakers with valuable insights into the potential impacts of different policy interventions on renewable energy adoption. By delineating distinct clusters of future trajectories based on HP adoption and PV production, we identify critical policy levers that can steer the residential sector towards sustainable energy transitions. For instance, the findings underscore the importance of maintaining incentives for both PV and HP installations to achieve ambitious renewable energy targets. Furthermore, the role of district heating policies emerges as a pivotal factor influencing HP penetration rates, highlighting the need for coordinated efforts to promote renewable heating solutions.

In conclusion, the integrated modeling framework presented in this study offers a powerful tool for policymakers and stakeholders to navigate the complexities of renewable energy adoption in the Ticino canton. However, it is imperative to acknowledge the evolving nature of technological innovation, regulatory frameworks, and societal preferences, necessitating continuous monitoring and adaptation of policies to align with changing dynamics.

Acknowledgement

The research published in this paper was carried out with the support of the Swiss Federal Office of Energy as part of the SWEET consortium SURE. The authors bear sole responsibility for the conclusions and the results presented.

References

[1] M. Chang, J. Z. Thellufsen, B. Zakeri, B. Pickering, S. Pfenninger, H. Lund, P. A. Østergaard, Trends in tools and approaches for modelling the energy transition, Applied Energy 290 (2021) 116731. doi:https://doi.org/10.1016/j.apenergy.2021.116731.
URL https://www.sciencedirect.com/science/article/pii/S0306261921002476

[2] M. Jaxa-Rozen, E. Trutnevyte, Sources of uncertainty in long-term global scenarios of solar photovoltaic technology, Nature Climate Change 11 (2021) 266–273. doi:https://doi.org/10.1038/s41558-021-00998-8.
URL https://www.nature.com/articles/s41558-021-00998-8

[3] X. Yue, S. Pye, J. DeCarolis, F. G. N. Li, F. Rogan, B. Gallachóir, A review of approaches to uncertainty assessment in energy system optimization models, Energy Strategy Reviews 21 (2018) 204–217. doi:https://doi.org/10.1016/j.esr.2018.06.003.
URL https://www.sciencedirect.com/science/article/pii/S2211467X18300543

[4] J. DeCarolis, H. Daly, P. Dodds, I. Keppo, F. Li, W. McDowall, S. Pye, N. Strachan, E. Trutnevyte, W. Usher, M. Winning, S. Yeh, M. Zeyringer, Formalizing best practice for energy system optimization modelling, Applied Energy 194 (2017) 184–198. doi:https://doi.org/10.1016/j.apenergy.2017.03.001.
URL https://www.sciencedirect.com/science/article/pii/S0306261917302192

[5] K. An, S. Zhang, J. Zhou, C. Wang, How can computable general equilibrium models serve low-carbon policy? A systematic review, Environmental Research Letters 18 (3) (2023) 033002, publisher: IOP Publishing. doi:10.1088/1748-9326/acbbe2.
URL https://dx.doi.org/10.1088/1748-9326/acbbe2

[6] E. Trutnevyte, L. F. Hirt, N. Bauer, A. Cherp, A. Hawkes, O. Y. Edelenbosch, S. Pedde, D. P. v. Vuuren, Societal Transformations in Models for Energy and Climate Policy: The Ambitious Next Step, One Earth 1 (4) (2019) 423–433. doi:https://doi.org/10.1016/j.oneear.2019.12.002.
URL https://www.sciencedirect.com/science/article/pii/S2590332219302246

[7] M. Yliruka, S. Moret, N. Shah, Detail or uncertainty? Applying global sensitivity analysis to strike a balance in energy system models, Computers & Chemical Engineering 177 (2023) 108287. doi:https://doi.org/10.1016/j.compchemeng.2023.108287.
URL https://www.sciencedirect.com/science/article/pii/S0098135423001576

[8] P.-H. Li, S. Pye, I. Keppo, M. Jaxa-Rozen, E. Trutnevyte, Revealing effective regional decarbonisation measures to limit global temperature increase in uncertain transition scenarios with machine learning techniques, Climatic Change 176 (2023). doi:https://doi.org/10.1007/s10584-023-03529-w.
URL https://doi.org/10.1007/s10584-023-03529-w

[9] A. T. D. Perera, F. Khayatian, S. Eggimann, K. Orehounig, S. Halgamuge, Quantifying the climate and human-system-driven uncertainties in energy planning by using GANs, Applied Energy 328 (2022) 120169. doi:https://doi.org/10.1016/j.apenergy.2022.120169.
URL https://www.sciencedirect.com/science/article/pii/S030626192201426X

[10] E. Pruyt, J. Kwakkel, G. Yücel, C. Hamarat, Energy transitions towards sustainability: A staged exploration of complexity and deep uncertainty, 29th International Conference of the System Dynamics Society, 2011.

[11] M. M. Dekker, V. Daioglou, R. Pietzcker, R. Rodrigues, H.-S. de Boer, F. Dalla Longa, L. Drouet, J. Emmerling, A. Fattahi, T. Fotiou, P. Fragkos, O. Fricko, E. Gusheva, M. Harmsen, D. Huppmann, M. Kannavou, V. Krey, F. Lombardi, G. Luderer, S. Pfenninger, I. Tsiropoulos, B. Zakeri, B. van der Zwaan, W. Usher, D. van Vuuren, Identifying energy model fingerprints in mitigation scenarios, Nature Energy 8 (2023) 1395–1404. doi:https://doi.org/10.1038/s41560-023-01399-1.
URL https://www.nature.com/articles/s41560-023-01399-1

[12] T. H. J. Inderberg, H. A. Nykamp, V. Olkkonen, E. Rosenberg, K. K. Taranger, Identifying and analysing important model assumptions: Combining techno-economic and political feasibility of deep decarbonisation pathways in Norway, Energy Research & Social Science 112 (2024) 103496. doi:https://doi.org/10.1016/j.erss.2024.103496.
URL https://www.sciencedirect.com/science/article/pii/S2214629624000872

[13] D. Süsser, H. Gaschnig, A. Ceglarz, V. Stavrakas, A. Flamos, J. Lilliestam, Better suited or just more complex? On the fit between user needs and modeller-driven improvements of energy system models, Energy 239 (2022) 121909. doi:https://doi.org/10.1016/j.energy.2021.121909.
URL https://www.sciencedirect.com/science/article/pii/S0360544221021575

[14] V. Heinisch, J. Dujardin, P. Gabrielli, P. Jain, M. Lehning, G. Sansavini, J.-P. Sasse, C. Schaffner, M. Schwarz, E. Trutnevyte, Inter-comparison of spatial models for high shares of renewable electricity in Switzerland, Applied Energy 350 (2023) 121700. doi:https://doi.org/10.1016/j.apenergy.2023.121700.
URL https://www.sciencedirect.com/science/article/pii/S0306261923010644

[15] B. Pickering, F. Lombardi, S. Pfenninger, Diversity of options to eliminate fossil fuels and reach carbon neutrality across the entire European energy system, Joule 6 (6) (2022) 1253–1276. doi:https://doi.org/10.1016/j.joule.2022.05.009.
URL https://www.sciencedirect.com/science/article/pii/S2542435122002367

[16] A. Nikas, A. Gambhir, E. Trutnevyte, K. Koasidis, H. Lund, J. Z. Thellufsen, D. Mayer, G. Zachmann, L. J. Miguel, N. Ferreras-Alonso, I. Sognnaes, G. P. Peters, E. Colombo, M. Howells, A. Hawkes, M. v. d. Broek, D. J. V. d. Ven, M. Gonzalez-Eguino, A. Flamos, H. Doukas, Perspective of comprehensive and comprehensible multi-model energy and climate science in Europe, Energy 215 (2021) 119153. doi:https://doi.org/10.1016/j.energy.2020.119153.
URL https://www.sciencedirect.com/science/article/pii/S036054422032260X

[17] C. Guivarch, T. L. Gallic, N. Bauer, P. Fragkos, D. Huppmann, M. Jaxa-Rozen, I. Keppo, E. Kriegler, T. Krisztin, G. Marangoni, S. Pye, K. Riahi, R. Schaeffer, M. Tavoni, E. Trutnevyte, D. v. Vuuren, F. Wagner, Using large ensembles of climate change mitigation scenarios for robust insights, Nature Climate Change 12 (2022) 428.435. doi:10.1038/s41558-022-01349-x.
URL https://doi.org/10.1038/s41558-022-01349-x

[18] F. J. Baader, S. Moret, W. Wiesemann, I. Staffell, A. Bardow, Streamlining Energy Transition Scenarios to Key Policy Decisions, _eprint: 2311.06625 (2023).

[19] A. Leopold, Energy related system dynamic models: a literature review, Central European Journal of Operations Research 24 (2016) 231–261. doi:https://doi.org/10.1007/s10100-015-0417-4.
URL https://doi.org/10.1007/s10100-015-0417-4

[20] E. Pruyt, J. Kwakkel, System dynamics and uncertainty, in: Proceedings of the International System Dynamics Conference, Delft, The Netherlands, 2014, pp. 20–24.

[21] F. G. N. Li, Actors behaving badly: Exploring the modelling of non-optimal behaviour in energy transitions, Energy Strategy Reviews 15 (2017) 57–71. doi:https://doi.org/10.1016/j.esr.2017.01.002.
URL https://www.sciencedirect.com/science/article/pii/S2211467X17300020

[22] L. S. Siegel, C. Campbell, A. Delibas, S. Eker, T. Fiddaman, T. Franck, J. Homer, A. P. Jones, C. Jones, J. Loughman, S. McCauley, E. Sawin, C. Soderquist, J. Sterman, En-ROADS Technical Reference, Climate Interactive, 2023.
URL https://docs.climateinteractive.org/projects/en-roads-reference-guide/en/latest/index.html

[23] E. Pruyt, T. Islam, T. Arzt, On the Spot and Map: Interactive Model-Based Policy Support Under Deep Uncertainty, in: J. R. Gil-Garcia, T. A. Pardo, L. F. Luna-Reyes (Eds.), Policy Analytics, Modelling, and Informatics: Innovative Tools for Solving Complex Social Problems, Springer International Publishing, Cham, 2018, pp. 315–342.

[24] J. H. Kwakkel, The Exploratory Modeling Workbench: An open source toolkit for exploratory modeling, scenario discovery, and (multi-objective) robust decision making, Environmental Modelling & Software 96 (2017) 239–250. doi:https://doi.org/10.1016/j.envsoft.2017.06.054.
URL https://www.sciencedirect.com/science/article/pii/S1364815217301251

[25] S. Mannucci, J. H. Kwakkel, M. Morganti, M. Ferrero, Exploring potential futures: Evaluating the influence of deep uncertainties in urban planning through scenario planning: A case study in Rome, Italy, Futures 154 (2023) 103265. doi:https://doi.org/10.1016/j.futures.2023.103265.
URL https://www.sciencedirect.com/science/article/pii/S0016328723001696

[26] F. G. N. Li, N. Strachan, BLUE: Behaviour Lifestyles and Uncertainty Energy model, Tech. rep., University College London (UCL) Energy Institute (2019).

[27] FOEN, Long-term climate strategy to 2050 (2021).
URL https://www.bafu.admin.ch/bafu/en/home/topics/climate/info-specialists/emission-reduction/reduction-targets/2050-target/climate-strategy-2050.html

[28] C. Camarasa, Mata, J. P. J. Navarro, J. Reyna, P. Bezerra, G. B. Angelkorte, W. Feng, F. Filippidou, S. Forthuber, C. Harris, N. H. Sandberg, S. Ignatiadou, L. Kranzl, J. Langevin, X. Liu, A. Müller, R. Soria, D. Villamar, G. P. Dias, J. Wanemark, K. Yaramenka, A global comparison of building decarbonization scenarios by 2050 towards 1.5–2 °C targets, Nature Communications 13 (1) (2022) 3077, publisher: Nature Publishing Group. doi:10.1038/s41467-022-29890-5.
URL https://www.nature.com/articles/s41467-022-29890-5

[29] C. Breyer, D. Bogdanov, A. Gulagi, A. Aghahosseini, L. S. Barbosa, O. Koskinen, M. Barasa, U. Caldera, S. Afanasyeva, M. Child, J. Farfan, P. Vainikka, On the role of solar photovoltaics in global energy transition scenarios, Progress in Photovoltaics: Research and Applications 25 (8) (2017) 727–745, _eprint: https://onlinelibrary.wiley.com/doi/pdf/10.1002/pip.2885. doi:10.1002/pip.2885.

URL https://onlinelibrary.wiley.com/doi/abs/10.1002/pip.2885

[30] F. Knobloch, H. Pollitt, U. Chewpreecha, R. Lewney, M. A. J. Huijbregts, J.-F. Mercure, FTT:Heat — A simulation model for technological change in the European residential heating sector, Energy Policy 153 (2021) 112249. doi:10.1016/j.enpol.2021.112249.
URL https://www.sciencedirect.com/science/article/pii/S030142152100118X

[31] Ventana Systems.
URL https://vensim.com/

[32] M. Castaneda, M. Jimenez, S. Zapata, C. J. Franco, I. Dyner, Myths and facts of the utility death spiral, Energy Policy 110 (2017) 105–116. doi:10.1016/j.enpol.2017.07.063.
URL https://www.sciencedirect.com/science/article/pii/S0301421517304949

[33] FSO, Register Buildings and Dwellings.
URL https://www.geocat.ch/geonetwork/srv/eng/catalog.search#/metadata/56553efe-4a2c-449d-93ba-cf7edd518d56

[34] SFOE, Electricity production plants.
URL https://www.geocat.ch/geonetwork/srv/eng/catalog.search#/metadata/e5a00bdb-5022-4856-ad4a-d1afe7bf38b0

[35] SFOE, Suitability of roofs for solar power.
URL https://www.geocat.ch/geonetwork/srv/eng/catalog.search#/metadata/b614de5c-2f12-4355-b2c9-7aef2c363ad6

[36] K. N. Streicher, P. Padey, D. Parra, M. C. Bürer, M. K. Patel, Assessment of the current thermal performance level of the Swiss residential building stock: Statistical analysis of energy performance certificates, Energy and Buildings 178 (2018) 360–378. doi:https://doi.org/10.1016/j.enbuild.2018.08.032.
URL https://www.sciencedirect.com/science/article/pii/S0378778818305875

[37] K. N. Streicher, P. Padey, D. Parra, M. C. Bürer, S. Schneider, M. K. Patel, Analysis of space heating demand in the Swiss residential building stock: Element-based bottom-up model of archetype buildings, Energy and Buildings 184 (2019) 300–322. doi:10.1016/j.enbuild.2018.12.011.
URL https://www.sciencedirect.com/science/article/pii/S0378778818325660

[38] ARE, Housing inventory and secondary homes rate.
URL https://www.geocat.ch/geonetwork/srv/ita/catalog.search#/metadata/ed80ebde-99a0-4523-bc8a-4ec23426d966

[39] FSO, Hedonic models 2023 - Swiss Residential Property Price Index - Yearly update of the quality adjustment | Publication (May 2023).
URL https://www.bfs.admin.ch/asset/en/24625176

[40] S. Müller, J. Rode, The adoption of photovoltaic systems in Wiesbaden, Germany, Economics of Innovation and New Technology 22 (5) (2013) 519–535, publisher: Routledge _eprint: https://doi.org/10.1080/10438599.2013.804333. doi:10.1080/10438599.2013.804333.
URL https://doi.org/10.1080/10438599.2013.804333

[41] T. H. Meles, L. Ryan, Adoption of renewable home heating systems: An agent-based model of heat pumps in Ireland, Renewable and Sustainable Energy Reviews 169 (2022) 112853. doi:10.1016/j.rser.2022.112853.
URL https://www.sciencedirect.com/science/article/pii/S1364032122007353

[42] TI, Regolamento sull'utilizzazione dell'energia (RUEn) (2024).
URL https://m3.ti.ch/CAN/RLeggi/public/index.php/raccolta-leggi/legge/num/526

[43] E. Quade, Analysis for public decisions, 1975.

[44] M. G. Morgan, M. Henrion, M. Small, Uncertainty: A Guide to Dealing with Uncertainty in Quantitative Risk and Policy Analysis, Cambridge University Press, 1990, google-Books-ID: ajd1V305PgQC.

[45] J. H. Kwakkel, W. E. Walker, V. A. Marchau, Classifying and communicating uncertainties in model-based policy analysis, International Journal of Technology, Policy and Management 10 (4) (2010) 299–315, publisher: Inderscience Publishers. doi:10.1504/IJTPM.2010.036918.
URL https://www.inderscienceonline.com/doi/abs/10.1504/IJTPM.2010.036918

[46] M. D. Morris, Factorial sampling plans for preliminary computational experiments (1991).

[47] A. Saltelli, M. Ratto, T. Andres, F. Campolongo, J. Cariboni, D. Gatelli, M. Saisana, S. Tarantola, Global Sensitivity Analysis: The Primer, John Wiley & Sons, 2008, google-Books-ID: wAssmt2vumgC.

[48] I. M. Sobol, Global sensitivity indices for nonlinear mathematical models and their Monte Carlo estimates, Mathematics and Computers in Simulation 55 (1) (2001) 271–280. doi:10.1016/S0378-4754(00)00270-6.
URL https://www.sciencedirect.com/science/article/pii/S0378475400002706

[49] Y. Tian, K. Hassmiller Lich, N. D. Osgood, K. Eom, D. B. Matchar, Linked Sensitivity Analysis, Calibration, and Uncertainty Analysis Using a System Dynamics Model for Stroke Comparative Effectiveness Research, Medical Decision Making 36 (8) (2016) 1043–1057, publisher: SAGE Publications Inc STM. doi:10.1177/0272989X16643940.
URL https://doi.org/10.1177/0272989X16643940

[50] D. Peel, G. MacLahlan, Finite mixture models (2000).

[51] B. P. Bryant, R. J. Lempert, Thinking inside the box: A participatory, computer-assisted approach to scenario discovery, Technological Forecasting and Social Change 77 (1) (2010) 34–49. doi:10.1016/j.techfore.2009.08.002.
URL https://www.sciencedirect.com/science/article/pii/S004016250900105X

[52] SE, Photovoltaikmarkt: Preisbeobachtungsstudie 2020, Tech. rep. (2020).

[53] JASM, Energy conversion technologies in STEM.
URL https://data.sccer-jasm.ch/energy-conversion-technologies-stem/2020-03-05/

[54] PdC, PdC-modulo di sistema - Pompe di calore efficienti con sistema.
URL https://www.wp-systemmodul.ch/it/

[55] Propellets, Propellets.
URL https://www.propellets.ch/it/riscaldare-con-il-pellet/cifre-e-fatti/prezzo-del-pellet

[56] Metanord, Metanord.
URL https://www.metanord.ch/wp-content/uploads/2022/08/Tariffario-fornitura-MSA-Validita-dal-01.10.2022.pdf

[57] S. Moret, Strategic energy planning under uncertainty, Ph.D. thesis, EPFL (2017). doi:10.5075/epfl-thesis-7961.

[58] EMap, Emissions of electricity consumption.
URL http://electricitymap.tmrow.co

[59] TI, Decreto Esecutivo 741.270 (2021).
URL https://m3.ti.ch/CAN/RLeggi/public/index.php/raccolta-leggi/legge/num/741

[60] OPEn, 730.03 - Ordinanza del 1° novembre 2017 sulla promozione della produzione di elettricità generata a partire da

energie rinnovabili (Ordinanza sulla promozione dell'energia, OPEn) (2017).
URL https://www.fedlex.admin.ch/eli/cc/2017/766/it

[61] TI, Bollettino Ufficiale 15/2022 (2022).
URL https://www3.ti.ch/CAN/RLeggi/public/index.php/raccolta-leggi/entrataVigore/

[62] J. Herman, W. Usher, SALib: An open-source Python library for Sensitivity Analysis, The Journal of Open Source Software 2 (9) (2017) 97. doi:10.21105/joss.00097.
URL http://joss.theoj.org/papers/10.21105/joss.00097

Appendix A. Model input data

Type	Performance	Vallemaggia	Mendrisio	Bellinzona	Leventina	Blenio	Lugano	Riviera	Locarno
SFH/DFH	Very Low	144	99	162	187	190	105	190	102
SFH/DFH	Low	119	82	134	154	157	86	152	83
SFH/DFH	Moderate	72	50	82	94	96	53	94	51
SFH/DFH	High	49	34	55	63	64	36	64	34
SFH/DFH	Very High	20	14	22	25	26	14	25	14
MFH	Very Low	115	69	113	148	151	74	136	74
MFH	Low	84	55	90	109	111	59	108	58
MFH	Moderate	57	39	64	73	75	41	75	40
MFH	High	36	25	41	47	48	26	48	26
MFH	Very High	20	13	22	25	26	14	26	14

Table A.5: Specific SH consumption [kWh/(m^2 year)] used as input in the model.

Variable	Unit	Use	Oil Boiler	Gas Boiler	Wood Boiler	Pellet Boiler	ST	HP	EH	PV
Capital cost [53]	CHF/kW	SFH/DFH MFH	1587 821	1460 756	2044 1764	2363 1764	8110 5661	2847 2180	730 378	f(kW) [52]
Fixed costs [53]	$CHF/kW/y$	SFH/DFH MFH	10.22 41.09	10.22 37.8	21.27 88.2	42.54 88.2	405.51 283.07	8.54 109	10.22 18.9	28.8 28.8
Lifetime [53]	years	SFH/DFH MFH	15 20	15 20	15 25	15 25	15 15	15 20	15 15	30 30
Efficiency [53]	-	SFH/DFH MFH	0.86 0.78	0.95 0.87	0.56 0.87	0.9 0.87	0.75 0.75	2.6 3.51	0.95 0.95	- -
Equivalent Hours [54]	h/y	SFH/DFH MFH	2200 1900	2200 1900	2200 1900	2200 1900	2200 1900	2600 2200	2200 1900	- -
Carrier cost	rp/kWh_{th}		14.4 [55]	16.2 [56]	4.8 [57]	13.8 [55]	-	Table	Table	-
GWP Cap	$kgCO_2eq/kW$		21.1	21.1	21.1	21.1	221.2	164.9	1.47	-
GWP Var	$kgCO_2eq/MWh$		331.5	267	11.8	11.8	-	117 [58]	117 [58]	-

Table A.6: Input data technologies

Variable	Unit	Pellet Boiler	ST	HP	PV
Inv Grant	CHF	5000 [59]	2500 [59]	7000 [59]	There are two contributions: - the federal one (”Remunerazione Unica” [60], 385 CHF + 420 CHF/kW) - the Cantonal one (”Contributo Unico” [61], 50 % of the ”Remunerazione Unica”)
Subsidy Cap	CHF/kW	100 [59]	500 [59]	180 [59]	

Table A.7: Incentives actually in force in Ticino.

Appendix B. Calibration results

Parameter	Optimal Value	Lower bound	Upper bound
β_1	0.0303	0.025	0.031
β_2	-2.118	-2.411	-2.040
β_3	16.287	15.740	16.425
β_0	-5.831	-5.920	-5.808
$\beta_{Vallemaggia}$	-0.589	-1.125	-0.143
$\beta_{Mendrisio}$	0.0035	-0.320	0.117
$\beta_{Bellinzona}$	-0.274	-0.921	-0.129
$\beta_{Leventina}$	-0.584	-1.198	-0.144
β_{Blenio}	-0.267	-0.863	0.207
β_{Lugano}	-0.052	-0.312	0.009
$\beta_{Riviera}$	-0.415	-0.948	-0.137
$\beta_{Locarno}$	0.601	0.220	0.696
$\beta_{VeryLow}$	-0.052	-0.266	0.026
β_{Low}	0.108	-0.206	0.189
$\beta_{Moderate}$	-0.214	-0.664	-0.131
β_{High}	0.071	-0.207	0.177
$\beta_{VeryHigh}$	-0.297	-0.622	-0.056
β_A	-0.218	-0.694	-0.095
β_B	0.340	0.124	0.383
β_C	-0.275	-0.444	-0.211
β_{SFH}	-0.054	-0.201	-0.024
β_{DFH}	0.339	-0.051	0.481
β_{MFH}	-0.039	-0.253	0.0971

(a) Calibrated parameters to compute Probability of Adoption PV and their 99% confidence interval bounds.

Parameter	Optimal Value	Lower bound	Upper bound
γ_1	-6.541	-5.850	-6.773
γ_2	45.258	49.520	39.282
γ_3	9.413	9.907	9.118
γ_4	-3.633	-3.251	-3.758
$\gamma_{Vallemaggia}$	-0.291	0.021	-0.699
$\gamma_{Mendrisio}$	-0.576	-0.232	-1.312
$\gamma_{Bellinzona}$	0.113	0.350	-0.314
$\gamma_{Leventina}$	-0.959	-0.336	-1.895
γ_{Blenio}	-0.759	-0.189	-1.474
γ_{Lugano}	0.054	0.177	-0.366
$\gamma_{Riviera}$	0.301	0.797	-0.354
$\gamma_{Locarno}$	0.391	0.591	0.007
$\gamma_{VeryLow}$	0.793	0.937	0.605
γ_{Low}	-0.882	-0.644	-1.433
$\gamma_{Moderate}$	-1.942	-1.817	-2.261
γ_{High}	1.076	1.302	0.306
$\gamma_{VeryHigh}$	-0.167	0.153	-0.476
γ_A	-0.742	-0.561	-1.271
γ_B	0.155	0.255	-0.127
γ_C	0.322	0.459	0.008
γ_{SFH}	0.231	0.300	0.035
γ_{DFH}	-0.045	0.217	-0.452
γ_{MFH}	-0.750	-0.553	-1.290

(b) Calibrated parameters to compute Probability of Adoption HP and their 99% confidence interval bounds.

Parameter	Optimal Value	Lower bound	Upper bound
ϕ	32.688	28.539	33.924
δ	0.564	0.540	0.708
ω	0.0268	0.540	0.070

(c) Calibrated parameters to compute the share of people considering PV and their 99% confidence interval bounds.

Category	PV r^2	HP r^2
SFH	0.94	0.36
DFH	0.86	0.42
MFH	0.91	0.53
A: < 150 m^2	0.89	0.31
B: 150-300 m^2	0.86	0.43
C: > 300 m^2	0.89	0.43
Vallemaggia	0.71	0.63
Mendrisio	0.80	0.39
Leventina	0.81	0.71
Bellinzona	0.90	0.38
Blenio	0.67	0.52
Lugano	0.91	0.31
Riviera	0.79	0.44
Locarno	0.87	0.47
Very Low	0.91	0.44
Low	0.87	0.47
Moderate	0.88	0.72
High	0.80	0.97
Very High	0.88	0.91

(d) Results of the calibration for each of the categories considered in terms of r^2 for both PV and HP

Table B.8: The for tables show the results of the calibration process explained in Section 2.1.4. In Tables (a), (b) and (c) are reported the optimal calibrated parameters and their confidence intervals; in Table (d) are shown the resulting r^2.

Appendix C. Morris GSA

In the application of the Morris screening method, considering a set of $k = 49$ input factors in the Global Sensitivity Analysis $\theta = \{\theta_1, \theta_2, ..., \theta_{49}\}$, let θ_i^{min} and θ_i^{max} denote the minimum and maximum possible values for parameter θ_i, respectively. θ_i is then defined as $\theta_i = \theta_i^{min} + l_i(\theta_i^{max} - \theta_i^{min})$, and l_i is taken with equal probability from the set $\left\{0, \frac{1}{h-1}, \frac{2}{h-1}, ..., 1\right\}$ [46]. Where h is the number of levels; this is assumed to be equal to 4, which is the default value assumed in the python SALib package [62], the one used to perform this analysis. Let $y(\theta)$ denote the model deterministic output y for a given set of θ values. In this way the elementary effect (EE_i) of θ_i on y is computed as:

$$EE_i(\theta) = \frac{y(\theta_1, ..., \theta_i + \Delta, ..., \theta_{49}) - y(\theta_1, ..., \theta_{49})}{\Delta} \tag{C.1}$$

where Δ is defined as a multiple of $\frac{1}{h-1}$. Starting from an initial base value for each θ_i selected at random from the uniform distribution between θ_i^{min} and θ_i^{max}, one random parameter θ_i is incremented or decremented and its elementary effect is calculated. From this next value, another random parameter θ_k is again incremented, and its elementary effect calculated and so on until we have calculated one elementary effect for each factor. This process is repeated r times, with the parameter r called replication of trajectories, which is assumed to be equal to 10 in this analysis. Following this procedure, a total of $r(k+1) = 500$ samples are generated and r elementary effects per input are computed, making it possible to find their average absolute value and standard deviation according to:

$$\mu_i^* = \frac{1}{r} \sum_{j=1}^{r} \left| EE_i^j \right| \tag{C.2}$$

$$\sigma_i = \sqrt{\frac{1}{r} \sum_{i}^{r} \left(EE_i^j - \frac{1}{r} \sum_{i}^{r} EE_i^j \right)^2} \tag{C.3}$$

Appendix D. Gaussian Mixture Model

The Gaussian Mixture Model (GMM) is a probabilistic model commonly used for clustering data. It assumes that the data points are generated from a mixture of several Gaussian distributions. Each Gaussian distribution represents a cluster in the data, and the model aims to identify these clusters by estimating the parameters of the Gaussians, including their means and covariances. It is advantageous because it is capable of identifying clusters with non-spherical shapes and can accommodate clusters of varying sizes and densities. Additionally, it provides probabilistic cluster assignments, allowing for uncertainty estimation in cluster assignments. However, it is important to note that the performance of the GMM can be sensitive to the initializations of number of clusters to be identified. Therefore, the Bayesian Information Criterion (BIC) and Akaike Information Criterion (AIC) are used as a criterion to identify the optimal number of clusters. These parameters, as shown in Figure D.7 are computed varying the number of clusters to be identifies: the optimal number of clusters is the one that minimizes the BIC and AIC, so in our case it is three.

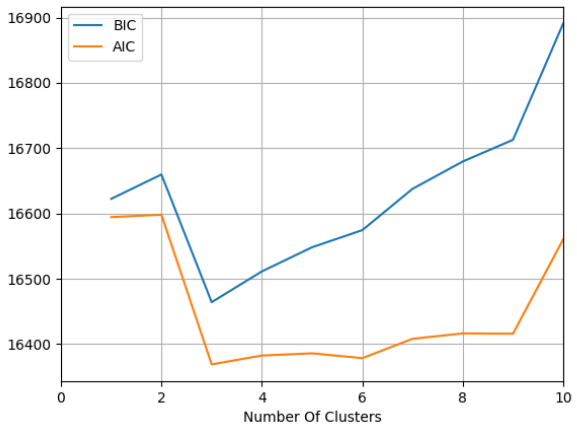

Figure D.7: Resulting BIC and AIC varying the number of clusters considered.

Appendix E. PRIM scenario discovery

Scenario discovery, increasingly employed to deal with uncertainties driving outcomes within extensive scenario ensembles, can make use of different data mining algorithms; one of the most used is the patient rule induction method (PRIM). PRIM seeks to identify sub-spaces within the uncertainty realm, representing combinations of uncertain input values leading to predefined regions in the outcome space. These outcome-driven sub-spaces, along with the associated uncertainty sub-spaces, distinguish themselves from others. An example is show in Figure E.8, where the PRIM analysis is applied to find the uncertain input ranges that lead to the outcomes in Cluster 1.

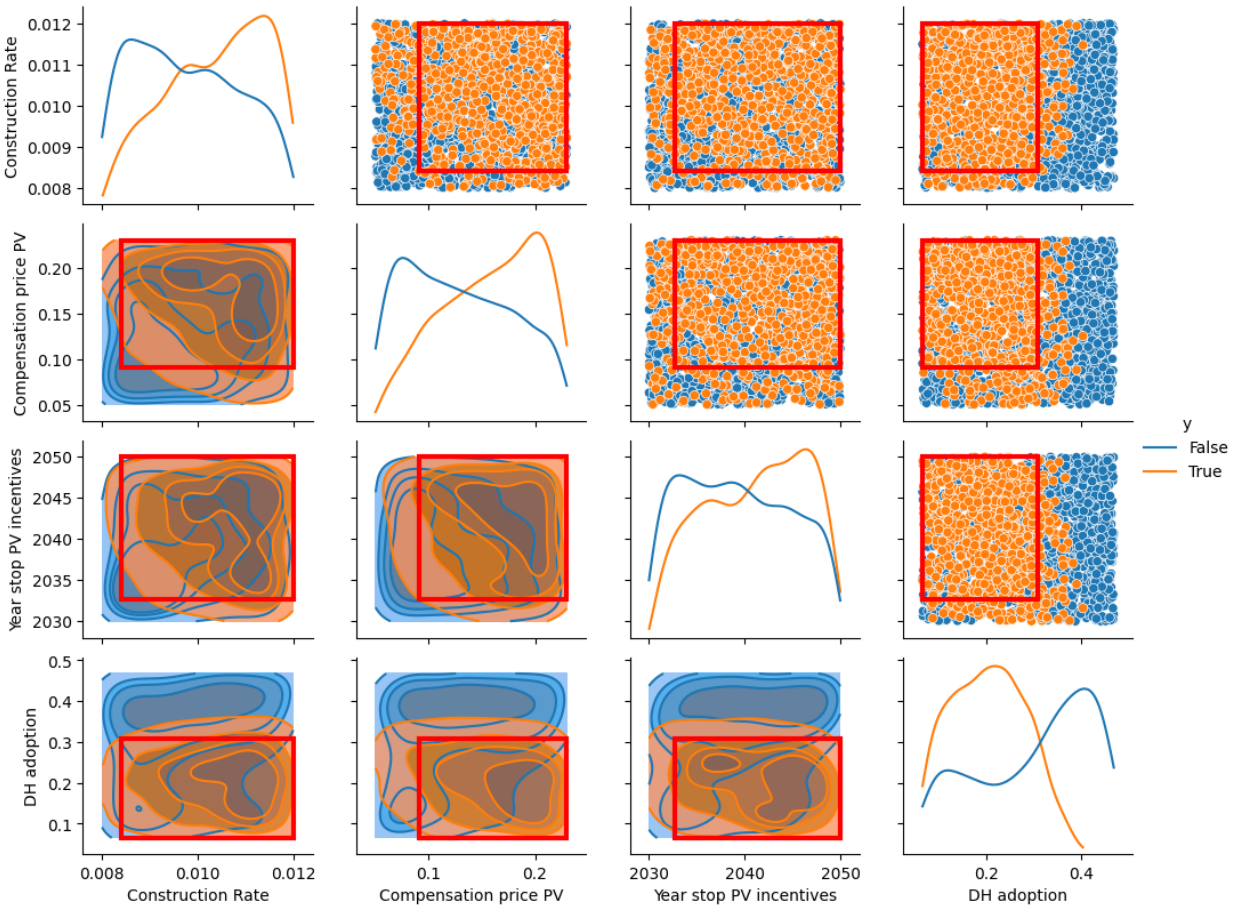

Figure E.8: Example of how PRIM works in order to find the range of input parameters that allow to result in the output of interest.

As indicated in Figure 6 each box exhibits two pivotal attributes: “density”, denoting the ratio of cases of interest within a box to the total cases, and “coverage”, representing the ratio of cases of interest in a box to the total cases of interest across the scenario space. While a high-density, high-coverage box is ideal, there often exists a trade-off between the precision conferred by density and the inclusiveness facilitated by coverage.

In our investigation, we utilized the PRIM implementation within the Python library Exploratory Modelling and Analysis (EMA) Workbench. This implementation not only provides coverage and density metrics for each box but also reports quasi P values indicating the likelihood of a parameter being constrained by chance. These P values, derived from a quasi P-test by Bryant and Lempert [51], evaluate the null hypothesis that the contribution of a restricted parameter to the box is negligible compared to that of all other restricted parameters within the box. Hence, small P values reject the null hypothesis, suggesting that a parameter is identified with a degree of confidence, not by coincidence.

We applied the PRIM algorithm to each of the three clusters identified through Gaussian Mixture Modeling (GMM). The resulting boxes in each PRIM execution demonstrate a near-linear trade-off between coverage and density for Clusters 1 and 2 (refer to Figures E.9b and E.9c), indicating that optimizing one metric may necessitate sacrificing the other, and a non linear trade-off for Cluster 0 (Figure E.9a). For simplicity, our analysis focused on one box per identified cluster. However, for a more comprehensive understanding of policy implications, it is recommended to conduct further PRIM analyses on multiple boxes.

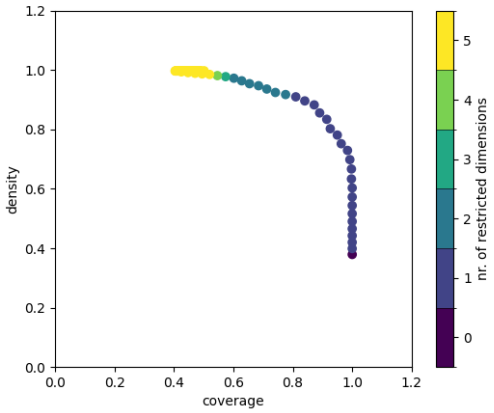

(a) Results for Cluster 0.

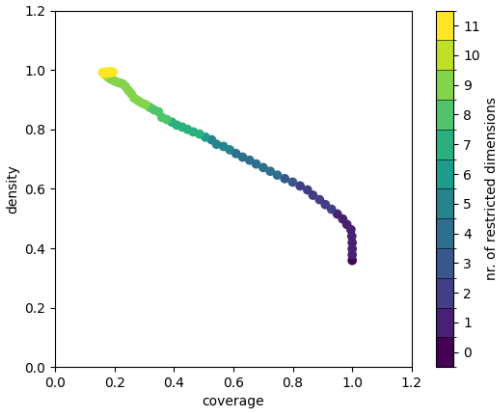

(b) Results for Cluster 1.

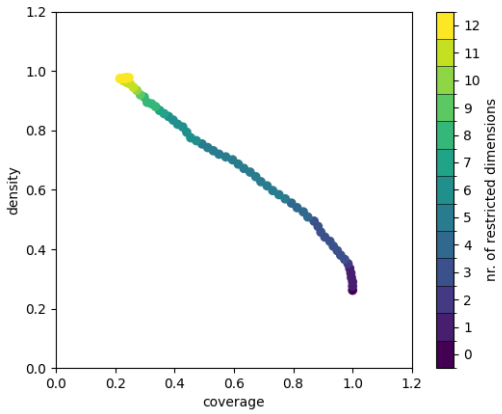

(c) Results for Cluster 2.

Figure E.9: Representation of the trade-offs associated with each cluster considered. Each point represents a possible box. If the restricted dimentions (i.e. the input ranges restricted) is null, the coverage is one, but the density is low: this means that the considered box comprehends all the outputs of interest, but that a high share of the scenarios in the box are not in the output of interest. If the restricted dimentions increase, the coverage decrease, but its density increases.